
A Foundation Graph Model

Alex O. Davies¹ Riku Green¹ Nirav Ajmeri¹ Telmo de Menezes e Silva Filho²

Abstract

The principal benefit of unsupervised graph representation learning is that a pre-trained model can be fine-tuned where data or labels are scarce. Existing approaches are domain specific, maintaining consistent node and edge attributes across the pre-training and target datasets. This precludes transfer to other domains. A model capable of positive transfer on arbitrary tasks and domains would represent the first foundation graph model.

In this work we use adversarial contrastive learning to present FoTOM, a graph pre-training method based on node and edge feature exclusion. We use FoTOM to pre-train models over multiple graph domains, producing the first foundation graph models. We demonstrate positive transfer on evaluation datasets from multiple domains, including domains not present in pre-training data. On all datasets performance is at worst on-par and on 76% significantly better than a supervised baseline, with an 8 to 40% reduction in error at 95% confidence. Contrary to other research, pre-training on a dataset with the target domain excluded leads us to better performance than pre-training on a dataset from only the target domain. The multi-domain model at worst, matches, and on 56% of tasks, significantly outperforms single-domain ($P \leq 0.01$). These results include when node labels are used in evaluation, where performance is consistently superior to single-domain or non-pre-trained models. Notably, FoTOM benefits scenarios in both large or scarce data regimes for the target domains.

alexander.davies@bristol.ac.uk

¹ School of Computer Science

² School of Engineering Mathematics and Technology
University of Bristol, UK

1. Introduction

Graph learning has received considerable attention in recent years (Zhou et al., 2020). Despite the success of foundation language models, the question of how to train a foundation

graph model remains open (Shirzad et al., 2022). Foundational language models have been trained through self-supervised representation learning. The success of these models is largely attributed to scaling up the size of data used for pre-training. Recent works for pre-trained graph models, where data-scaling is limited to just one domain, are yet to adopt this approach. The principle obstacle has been maintaining consistent node and edge features across the pre-training and downstream datasets. In order to develop graph foundation models, methods to scale graph data to multiple domains must be explored.

Graphs are a challenging form of data to process, given their high dimensionality. Methods normally applied to continuous or categorical data-types cannot be easily transferred to the graph domain. As such much work has been conducted on forming useful representations of graphs which are more easily used by well explored methods. Khoshraftar et al. (2022), Hamilton et al. (2017) and Chen et al. (2020) provide surveys on graph representation learning in general. These and other works focus on in-domain learning, where a single model is pre-trained and fine-tuned on data from a single domain. The principle motivation for this approach is maintaining consistent node and edge features between pre-training and downstream tasks. To the best of our knowledge there have been no works proposing to learn representations for multiple domains of graphs.

In this work we present FoTOM (**F**oundation **T**opology **M**odels), a generalised pre-training method for graph models, which relies on excluding node and edge features. We create a multi-domain dataset, and using FoTOM through contrastive learning, produce pre-trained models with consistently positive transfer on multiple domains. Under recent definitions these are the first foundation graph models (Bomasani et al., 2021; Liu et al., 2023; Zhang et al., 2023).

1.1. Hypotheses

We take the definition of a ‘foundation model’ from Bomasani et al. (2021), a definition since used by broad sources including world governments (Competition and Markets Authority, 2023), as “a type of AI technology . . . can be adapted to a wide range of tasks and operations”. Our interpretation given this definition is a single model that can be transferred with broadly positive performance increases on arbitrary

graph tasks. From this, we present our two hypotheses:

Hypothesis 1 (H1): There are useful generic structures within graphs, excluding node and edge features, that can be applied across domains.

Hypothesis 2 (H2): With the exclusion of node and edge features out-of-domain pre-training can have greater benefits than in-domain pre-training.

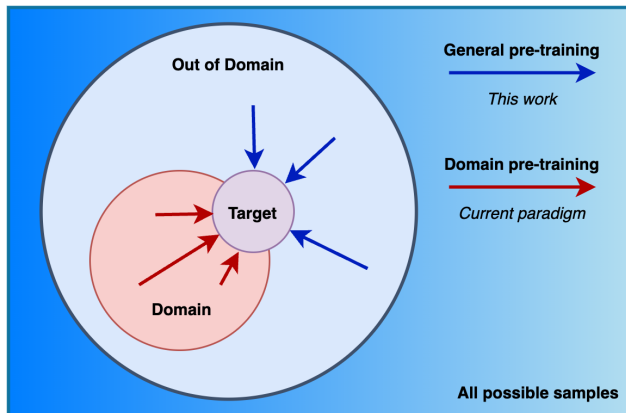


Figure 1: Current graph pre-training is domain-specific, with transfer only to near-domain samples, in order to maintain consistency for node and edge features.

Contribution Our contribution, following these hypotheses, is a method for generalised pre-training of graph models. Our method, FoToM, relies on the exclusion of node and edge features during pre-training. In the interest of simplicity we use only node and edge labels as features. These are excluded during pre-training. We evaluate our method using graph contrastive learning with both random and adversarial augmentations. Through this evaluation we present the following findings:

1. Pre-training on varied domains, under the exclusion of node and edge features, leads to positive transfer.
2. Pre-training in this manner is more beneficial from varied non-target domains than from the target domain.

Both of these findings go beyond the current consensus of graph pre-training, opening broad avenues of research and application. In particular the second finding directly opposes the current single-domain training paradigm.

Through the first finding we find that under fine-tuning results at worst on-par, and on 76% of tasks significantly better, than a non-pretrained baseline. At 95% confidence we observe a reduction in error of 8 to 40%. For the second finding results are similar. On molecular benchmarks we find that a model pre-trained on non-molecules, compared to pre-trained only on molecules, is at worst on-par. On 56% of tasks the non-molecule model performs significantly better, with 1 to 21% comparative decrease in error at 95% confidence.

2. Background

Here we define the notation and concepts necessary to understand the rest of this work. We then delineate the broad state of graph representation learning and the current obstacles to foundation graph models.

Representation Learning Let the input random variable $X \in \mathcal{X}$ represent data points in the input space \mathcal{X} . Similarly, the output random variable $Y \in \mathcal{Y}$ corresponds to the output space \mathcal{Y} , which is often the target space. Given their joint distribution $p(X, Y)$, the relevant information is defined as the mutual information $I(X; Y)$. Let F denote a mapping $X \rightarrow \hat{X}$; finding an optimal representation \hat{X} is formulated as minimising the following Lagrangian (Tishby and Zaslavsky, 2015):

$$L[p(\hat{x}|x)] = I(X; \hat{X}) - \beta I(\hat{X}; Y) \quad (1)$$

For unsupervised representation learning, the function F is learnt without supervision on Y .

Contrastive Learning It is possible to make progress in minimising Equation 1 via contrastive learning (Suresh et al., 2021). Let \mathcal{T} denote a set of augmentation functions where $t \in \mathcal{T} : X \rightarrow X'$. Intuitively these functions make small alterations to the input sample. An encoder $F(\cdot)$ maps between X and \hat{X} . From this encoding a projection head $g(\cdot)$ maps from \hat{X} and Z . A sample X undergoes two distinct augmentations, $X \rightarrow X', X''$, and in combination the encoder and projection head are trained to maximize agreement between Z for both augmented samples using a contrastive loss. After training is completed the encoder $F(\cdot)$ and representation \hat{X} are used for downstream tasks.

Graphs Let $G = (V, E)$, an un-attributed graph (topology) with node set $V = \{v_1, v_2, \dots, v_n\}$ and edges between them $E = \{(v_1, v_3), (v_2, v_4), \dots\}$. Let $n = |V|$ and $m = |E|$ denote the number of nodes and edges respectively. Let $X_V \in \mathbb{R}^{n \times d_V}$ denote the initial node feature matrix, where each node $i \in V$ has numeric vector node features of dimension d_V . Similarly edge features are denoted $X_E \in \mathbb{R}^{m \times d_E}$. With the inclusion of features and a graph-level label y a graph is $\underline{G} = (V, E, X_V, X_E, y)$. As an example a molecule might have V as atoms, E as bonds between these atoms, X_V atom labels and calculated features, X_E bond types and counts, and y a molecular property such as solubility.

2.1. Related Work

Graph Representation Learning Hamilton (2020) provides a comprehensive summary of methods for Graph Representation Learning (GRL). Traditional methods to encode graphs as vectors include graph statistics such as centrality measures and clustering coefficients, but also ker-

nel methods such as the Weisfeiler-Lehman (WL) kernel (Schweitzer PASCAL et al., 2011). Expressive Graph Neural Networks (GNNs) models, generally through parameterised message-passing, can produce powerful representations of graphs. A number of GNN architectures have been proposed with the Graph Isomorphism Network (GIN) being the most expressive (Zhou et al., 2020).

Graph Contrastive Learning Multiple studies exist for graph contrastive learning (Chu et al., 2021; Hafidi et al., 2022; Hassani and Khasahmadi, 2020; Hu et al., 2020; Li et al., 2021; You et al., 2020; Zhu et al., 2021). The typical graph contrastive learning formulation, GraphCL, is put forwards by (You et al., 2020). They propose or describe four different graph augmentation strategies: **1)** Node dropping, in which a subset of nodes are removed. **2)** Edge perturbation, in which edges are added or removed. **3)** Attribute masking, in which some subset of features are removed. **4)** Subgraph sampling, in which subgraphs are used as augmentations. In GraphCL work and many subsequent works, such augmentations are performed randomly using fixed parameters, ie ‘drop 20% of nodes’.

Adversarial Graph Contrastive Learning It has been shown that the quality of augmentations is critical for GCL (Zhu et al., 2021; You et al., 2020). To maximise expressivity in these augmentations adversarial strategies have been proposed (Hassani and Khasahmadi, 2020; Zhao et al., 2023). Suresh et al. (2021) propose Adversarial-Graph Contrastive Learning (AD-GCL), with their method training both an encoder and a ‘view-learner’. The idea is to perform the standard GCL protocol with weight updates to a parameterised set of augmenting functions \mathcal{T} through the contrastive loss. Here \mathcal{T} learns augmentations that minimise mutual information between the source and augmented graphs through edge dropping. The encoder, adversarially to this, learns to maximise shared information between the respective augmentations. The updates for \mathcal{T} are regularised such that augmentations are not entirely destructive.

Graph Foundation Models Whilst improvements have been made towards contrastive learning methods, little work has been completed in methodologies to combine different domains of graph data effectively. Ubiquitous in other fields, primarily text and images, is pre-training on a large amalgamated dataset of samples. Archetypal to this approach is ImageNet (Russakovsky et al., 2015), a massive combined dataset of images that aims to span the full space of realistic or likely images. Previous authors have argued, but not shown, that an ImageNet equivalent for graphs is not feasible (Shirzad et al., 2022). Such an approach has been discussed in recent literature by Zhang et al. (2023). In this work the authors argue that the ‘*extreme diversity*’ present in graph data make producing a graph foundation model for multiple graph domains ‘*exceedingly challenging*,

if not unlikely’. The assumption in this and prior works has been that the presence of node and edge attributes, with greatly varied meaning between domains, precludes generalised pre-training on an amalgamated dataset. We argue that this commitment to consistent features between pre-training and downstream tasks is the principle obstacle to the scale required for foundation models.

3. Method

Here we describe our method for evaluating FOTOM, a method for generalised pre-training of graph models. Using FOTOM node and edge features are excluded during pre-training This means an encoder is pre-trained on only the topology G , without the features or labels present in \underline{G} . This treatment of graphs G as abstract structures, instead of specific examples, allows creation of a multi-domain amalgamated dataset. Recent works view the creation of such a graph dataset, given node and edge features, as unfeasible (Shirzad et al., 2022; Liu et al., 2023; Zhang et al., 2023).

3.1. Excluding Features

Establishing Hypothesis 1 requires producing a model that has learnt useful representations of graphs *in general*. Our first step to achieving this is to construct a dataset that covers a reasonable breadth of real-world graphs. Constructing a dataset of real-world graphs is itself a reasonable narrowing of scope, but as the possible space of graphs at each number of nodes is so massive, constraining ourselves to a large and highly varied set of graphs is a reasonable step. Such a dataset should contain graphs that present a large diversity of multi-node patterns. Our approach is simple: include graphs from many domains, and assume that there is adequate coverage of the multi-node patterns that occur in real-world graphs. The same approach has essentially been taken in the domains of text (Brown et al., 2020) and images (Rombach et al., 2022), where enormous numbers of data samples are scraped from the web for generative pre-training. This relies on the assumptions that **a)** this dataset adequately covers the relevant space, and **b)** a single model can learn such a broad space. This assumption, as in other fields, is evaluated through downstream tasks on seen and unseen domains.

We formulate our test for Hypothesis 1 as beating a simple supervised baseline. Said baseline is a model with the same architecture as the pre-trained model but without pre-training. Both models are then trained, or fine-tuned for the pre-trained model, on the same downstream datasets under the same conditions. On each downstream task, should the pre-trained model match or out-perform the supervised model, this represents positive transfer. Positive transfer on a task indicates that at least some of the learning during pre-training was beneficial to subsequent learning during fine-tuning. A positive transfer rate across datasets of more

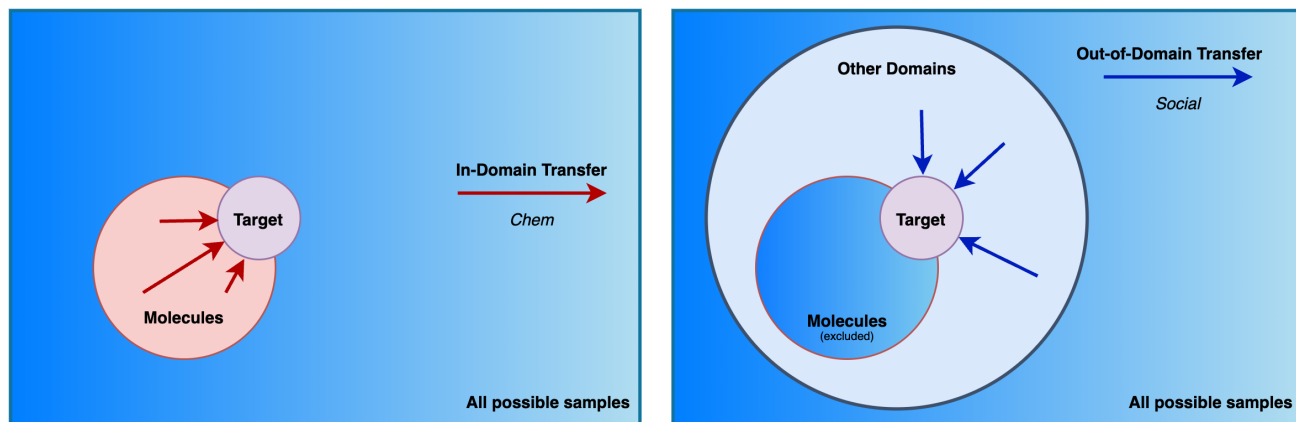


Figure 2: The Chem model is pre-trained only on molecular data, meaning in-domain transfer onto molecular datasets. The Social model is pre-trained only on non-molecular data, meaning out-of-domain transfer onto molecular datasets.

than 50% indicates that in-general transfer is positive, thus meeting the minimum criteria for Hypothesis 1. A high positive transfer rate would strongly establish Hypothesis 1.

3.2. Data Subsets

In order to evaluate Hypothesis 2, that domain diversity brings greater benefits than samples from the same domain, we need to produce models trained under different subsets of our data. The first model (Domain Model) is trained on a dataset from a single domain, as is the current status-quo. Said single domain matches that of the downstream target dataset(s). The second (Diverse Model) is instead trained on the rest of the data *while excluding the target domain*. The total size of the pre-training datasets for each model should match for fair comparison. By pre-training both models under the same controlled conditions (hyperparameters etc.), then evaluating their performance under fine-tuning, we can directly compare pre-training on a single domain to pre-training on multiple domains. A simple diagram for this process, specific to the experiments detailed in the next section, is presented in Figure 2.

In order to evaluate Hypothesis 2 we can apply both models on the given target domain. Verifying that Hypothesis 2 holds requires that positive transfer rates should be higher from the Diverse Model than from the Domain Model. The minimum threshold here is on-par positive transfer rates from each model. General positive transfer from the Diverse Model, and general negative transfer from the Domain Model, would constitute a clear result for Hypothesis 2.

4. Experiments

We begin by collating a collection of graph datasets. The datasets we use are described in aggregate measurements in Table 1. **molpcba** (Hu et al., 2020) A dataset of

437,929 small molecules selected from MoleculeNet (Wu et al., 2017). **molesol**, **molreesolv**, **mollipo**, **molclintox**, **molbbbp**, **molbase**, **molhiv** (Hu et al., 2020) Smaller datasets sampled from MoleculeNet, with single-target classification or regression downstream tasks. **Facebook** (Rozenberczki et al., 2021) A single graph of page-page connections on Facebook. Originally 22,470 nodes and 171,002 edges. Downstream task set to be predicting average clustering. **Twitch** (Rozenberczki et al., 2020) Ego networks from the streaming platform Twitch. Ego networks have one central “hub” node, which shares an edge with all other nodes. This dataset has a downstream binary classification task. **Cora** (McCallum et al., 2000) A much used citation graph. 2,810 nodes and 7,981 edges. Downstream task set to be predicting the number of 4-cycles in the graph normalised by graph size. **Roads** (Leskovec et al., 2009) The road network of Pennsylvania. Junctions are nodes, of which there are 1,088,092, with edges roads between them, of which there are 1,541,898. Downstream task set to be predicting graph diameter normalised by graph size. **Fly Brain** (Winding et al., 2023) The full neural connectome of a fruit fly larvae. Each node is a neuron, of which there are 3,016. Each edge is a synapse between neurons, but as the multi-graph is dense at originally 548,000 edges, we only include an edge between neurons if there are more than two synapses between them. Downstream task set to be predicting the number of 5-cycles in the graph normalised by graph size. **Trees** Trees, of a randomly sampled maximum depth, and a randomly fixed probability of branching at each level. Downstream tasks is predicting depth. **Random** Random Erdos-Renyi (ER) graphs (Erdos and Renyi, 1960), with a number of nodes and edge probability randomly sampled. These could represent noise during training, but predicting edge probabilities from embeddings represents a useful bare-minimum downstream task during validation and testing. **Community** Small ER subgraphs, with a set intra-subgraph

A Foundation Graph Model

Table 1: Statistics for each of our datasets. If used for training, we denote these statistics averaged across the training data. Otherwise we report statistics for their validation (downstream fine-tuning) datasets. ‘BC’ indicates binary classification.

	Num. Graphs	Number of Nodes	Number of Edges	Diameter	Avg. Clustering	Task Desc.
Training Only						
molpcba	250000	25.7 ± 6.28	27.7 ± 7	13.5 ± 3.29	0.00128 ± 0.0115	—
Training and Evaluation						
Twitch	50000	29.6 ± 11.1	86.6 ± 70.7	2 ± 0	0.549 ± 0.149	BC. Games Played
Facebook	50000	59.5 ± 20.7	206 ± 170	10.2 ± 6.39	0.429 ± 0.133	Avg. Clustering
Cora	50000	59.3 ± 20.7	119 ± 56.6	10.1 ± 4.68	0.322 ± 0.0845	Num. 4-Cycles
Roads	50000	59.5 ± 20.8	73.9 ± 28.2	16.4 ± 5.92	0.0559 ± 0.0426	Diameter / V
Fly Brain	50000	59.5 ± 20.8	146 ± 99.6	8.8 ± 3.49	0.237 ± 0.0875	Num. 5-Cycles
Evaluation Only						
molesol	1015	12.7 ± 6.64	12.9 ± 7.62	6.81 ± 3.30	0.000353 ± 0.00417	Water Solubility
molreesolv	577	8.46 ± 3.97	8.02 ± 4.50	5.02 ± 2.09	0 ± 0.0	Solvation
mollipo	3780	27.0 ± 7.44	29.4 ± 8.22	13.8 ± 4.03	0.00366 ± 0.017	Lipophilicity
molclintox	1329	26.3 ± 15.8	28.0 ± 17.1	12.4 ± 6.09	0.00259 ± 0.0191	BC. Toxicity
molbbbp	1835	23.5 ± 9.89	25.4 ± 11.0	11.2 ± 4.03	0.00284 ± 0.0278	BC. Penetration
molbase	1361	34.0 ± 7.89	36.8 ± 8.13	15.2 ± 3.14	0.00672 ± 0.0205	BC. Bioactivity
molhiv	37014	25.3 ± 12.0	27.3 ± 13.1	12.0 ± 5.15	0.00158 ± 0.0156	BC. Inhibition
Evaluation Only, Unseen Domain						
Trees	5000	19.6 ± 6.96	18.6 ± 6.96	10.1 ± 3.11	0 ± 0	Depth
Random	5000	29.3 ± 10.7	111 ± 82.1	3.88 ± 1.16	0.227 ± 0.0998	Density
Community	5000	48 ± 0	323 ± 26.2	3 ± 0.0346	0.408 ± 0.0256	Inter-Comm. Density

edge probability and a random inter-subgraph connection probability, with inter-subgraph connectivity as target.

As the Facebook, Cora, Roads and Fly Brain datasets consist of a single graph, we employ Exploration Sampling With Replacement (Davies and Ajmeri, 2022) to construct datasets of many smaller graphs. We use a randomly selected exploration sampler¹ for each sample, which in turn samples a random number of nodes in the range $24 \leq |V| \leq 96$ from the source graph. The use of a selection of exploration samplers should further ensure that a large variety of graphs and topological features are included in the datasets.

Taking downstream task on each validation set where available, we simply sum their relevant scores (MSE and 1-AUROC) as a crude monitor for the model’s representational abilities. Taking 50,000 samples for each training set and 5,000 for the validation sets (molhiv is excluded here), we conduct a limited Bayesian hyperparameter sweep. The heuristic used is a simple summing of evaluation scores on each dataset weighted by the number of samples in that dataset. Taking these hyper-parameters we fit an AD-GCL model on the large dataset (‘All’, i.e. all domains), a second only on molecules (‘Chem’), and a third only on non-molecular graphs (‘Social’). We train each model for 100 epochs with a batch size of 512. We present a UMAP embed-

¹Metropolis Hasting Random Walk, Diffusion and Forest Fire samplers, from <https://little-ball-of-fur.readthedocs.io/en/latest/>

ding of encodings of the validation datasets for an untrained model, and the trained models, in Figure 3. Figure 4 shows the same for PCA projections in the Supplemental Material.

4.1. Models

Graph level tasks, including during validation during training, can be conducted using the embeddings z that during training are passed to the projection head g . In our evaluation of transfer learning, for each model and transfer process, we present results for both with and without node labels in the fine-tuning data. We include a simple diagram in Figure 8. This should indicate whether the transformations learnt by the encoder can be quickly re-tooled for applications where node labels contain essential data. The assumption here would be that FoToM has learnt graph structures in-general, and that under transfer the further complexity of node labels within this structure can be learnt more quickly.

We perform a limited ablation study by evaluating multiple models: **1) GIN**, an untrained GIN model of identical architecture. **2) Chem**, an AD-GCL model fit only on molecular datasets. **3) Social**, an AD-GCL model fit only on non-molecular datasets. **4) All**, an AD-GCL model fit on all the training data. **5) All (Random)**, a model trained with the loss function from (You et al., 2020) using random edge dropping. All models we employ are GIN layers with single linear layers as input and output. The GIN model acts as our supervised baseline (Hypothesis 1). The Chem/Social

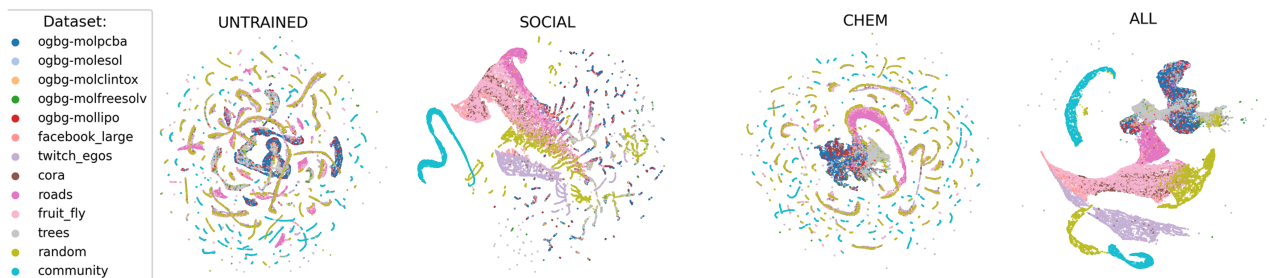


Figure 3: A UMAP embedding of encodings from each model, as well as an untrained model. The untrained and Chem models are noticeably more fragmented than the Social and All models. In turn the Social model is more fragmented than the All model. In the All model embedding, molecules are all in the same region, furthest from the Twitch Ego networks, with the Cora and Facebook Page-Page data “filling the gap”.

models indicate the impact of training data diversity on downstream transfer performance, particularly on our downstream molecular datasets (Hypothesis 2). The All (Random) model shows the impact of adversarial augmentations. We also perform this analysis for random node dropping. These results can be found in the supplemental material.

4.2. Transfer

Here we apply our pre-trained models to various downstream tasks. We briefly detail simple linear transfer, then use full transfer (ie fine-tuning) as detailed in our Method.

Linear-Transfer We take 95% splits of the validation dataset and use the encodings to fit linear models for the downstream tasks. Recorded performance is evaluated using the whole corresponding test-set with 10-fold error bounds. The results are shown in the Supplemental material in Table 4. We find that for the majority of datasets the model trained on the whole dataset (“All”) out-performs the others.

Fine-Tuning A more complex transfer process, and in practise more likely than simply using linear models, is fine-tuning on downstream tasks and datasets. To this end we replace the projection head with a simple two-layer MLP, with a single output node. We then perform 10 fine-tuning runs on each validation dataset, with and without node labels, for each pre-trained model. The results of this transfer and fine-tuning are presented in Table 2.

The All model consistently out-performs the other models under fine-tuning on the majority of datasets. At $P \leq 0.01$ the All model significantly out-performs the GIN baseline on 76% of datasets. With a 95% confidence interval we observe 8 to 40% reduction in error. When performance is not significantly better, it is never significantly worse. Notably the All model always out-performs the All (Random) model, indicating the merits of using a learnt augmentation scheme in this multi-domain setting. Random node dropping (see Supplemental Material) also consistently performs worse than learnt augmentations.

The standard deviation of the results on each dataset are far lower than those for the non-pre-trained model and the domain-specific pre-trained models. In Figure-(6) in the supplemental material we show validation loss on the several datasets during fine-tuning for the All model and an un-pre-trained GIN with the same architecture. Here the advantages of pre-training are clear: the pre-trained model has consistently lower validation loss, seems to plateau later and at a lower loss, and has a far lower deviation in that loss than the baseline GIN. Interestingly this is true on the chemical tasks where node labels are essential.

Comparing all training methods, data subsets and whether labels are included (see Table 7 in the Supplemental material) is illustrative of the benefits of training on a wide range of topologies. Across all datasets models adversarially trained on the whole data out-perform supervised baselines. This is the core prerequisite for foundation-model status.

Pre-training only on molecules (‘Chem’ data subsets) results at-best on-par transfer compared to the supervised GIN baseline, with negative transfer on the large majority of datasets. Pre-training only on non-molecules, in comparison, results in positive transfer on the large majority of datasets and pre-training methods. At $P \leq 0.01$ the Social model significantly out-performs the Chem model on 57% of datasets. With a 95% confidence interval we observe 1 to 21% lower error from the Social model compared to the Chem model. As before, where performance is not significantly better, it is never significantly worse. We find that under pre-training with random edge dropping, effectively non-adversarial AD-GCL, performance actually drops when including molecular data (‘Social’ vs ‘All’). This suggests either that the learnt-views paradigm from AD-GCL is able to differentiate between molecules and non-molecules, and therefore apply different augmentations, or in-fact that a variety of non-molecular graphs in-general provides a more solid pre-training foundation than including molecules.

Table 2: Scores for fine-tuning the complete model on each validation dataset, with (**Model**-labels) and without (**Model**) node labels. We also include a model trained on all the data but with random edge dropping as augmentations, in the style of GraphCL (You et al., 2020). For the classification datasets we report AUROC and for regression datasets RMSE. Some datasets, where results are very similar for each model, are excluded. **Bold** text indicates a result beats the unsupervised (GIN) baseline. **Underlined** text indicates a superior result, down to three significant figures. Checkmarks \checkmark indicate that the All model significantly out-performs the GIN baseline at $P \leq 0.01$.

	GIN (Baseline)	All (Random Edges)	Chem	Social	All	
molreesolv	4.978 \pm 0.479	4.197 \pm 0.095	3.888 \pm 0.207	3.829 \pm 0.114	4.255 \pm 0.029	\checkmark
molesol	1.784 \pm 0.094	1.571 \pm 0.059	1.439 \pm 0.089	1.472 \pm 0.042	1.308 \pm 0.034	\checkmark
mollipo	1.129 \pm 0.040	1.068 \pm 0.026	1.041 \pm 0.019	0.989 \pm 0.010	0.967 \pm 0.014	\checkmark
molclintox	0.530 \pm 0.042	0.461 \pm 0.029	0.514 \pm 0.029	0.501 \pm 0.053	0.548 \pm 0.110	
molbbbp	0.565 \pm 0.043	0.603 \pm 0.029	0.544 \pm 0.043	0.600 \pm 0.026	0.589 \pm 0.022	
molbace	0.677 \pm 0.053	0.756 \pm 0.030	0.631 \pm 0.128	0.745 \pm 0.025	0.707 \pm 0.017	
molhiv	0.355 \pm 0.059	0.501 \pm 0.135	0.540 \pm 0.133	0.640 \pm 0.047	0.657 \pm 0.044	\checkmark
Facebook	0.311 \pm 0.065	0.237 \pm 0.063	1.17 \pm 0.165	0.133 \pm 0.003	0.134 \pm 0.002	\checkmark
Twitch Egos	0.72 \pm 0.006	0.739 \pm 0.007	0.689 \pm 0.021	0.736 \pm 0.005	0.79 \pm 0.006	\checkmark
Roads	0.46 \pm 0.073	0.252 \pm 0.029	0.571 \pm 0.065	0.104 \pm 0.001	0.103 \pm 0.000	\checkmark
Trees	0.203 \pm 0.012	0.187 \pm 0.020	0.242 \pm 0.025	0.115 \pm 0.000	0.117 \pm 0.001	\checkmark
Community	0.743 \pm 0.106	0.314 \pm 0.069	0.715 \pm 0.130	0.016 \pm 0.001	0.017 \pm 0.000	\checkmark
Random	0.529 \pm 0.228	0.289 \pm 0.098	0.589 \pm 0.089	0.044 \pm 0.000	0.044 \pm 0.000	\checkmark
	GIN-Labels	All (Random)-Labels	Chem-Labels	Social-Labels	All-Labels	
molreesolv	4.854 \pm 0.513	4.163 \pm 0.069	3.825 \pm 0.123	3.817 \pm 0.070	4.250 \pm 0.047	\checkmark
molesol	1.707 \pm 0.073	1.597 \pm 0.059	1.460 \pm 0.079	1.494 \pm 0.065	1.302 \pm 0.030	\checkmark
mollipo	1.143 \pm 0.031	1.063 \pm 0.038	1.704 \pm 0.033	0.992 \pm 0.009	0.974 \pm 0.012	\checkmark
molclintox	0.497 \pm 0.038	0.475 \pm 0.031	0.517 \pm 0.027	0.548 \pm 0.085	0.575 \pm 0.075	
molbbbp	0.561 \pm 0.034	0.589 \pm 0.031	0.551 \pm 0.042	0.595 \pm 0.029	0.616 \pm 0.019	\checkmark
molbace	0.698 \pm 0.050	0.744 \pm 0.034	0.594 \pm 0.110	0.722 \pm 0.045	0.716 \pm 0.023	
molhiv	0.626 \pm 0.052	0.479 \pm 0.102	0.469 \pm 0.098	0.653 \pm 0.047	0.642 \pm 0.040	
Facebook	0.749 \pm 0.250	0.263 \pm 0.067	1.19 \pm 0.250	0.140 \pm 0.008	0.134 \pm 0.001	\checkmark
Superior Result	0%	14.3%	0.0%	38.1%	66.7%	
Positive Transfer	-	85.7%	38.1%	95.2%	100%	

5. Discussion

Here we discuss our findings in terms of our Hypotheses. This includes discussion on the performance of, and reasonable use cases for, models trained with FoTOM. Finally we detail explicitly significant assumptions we have made and potential risks to the validity of this work.

5.1. Findings

Our review of the field shows that maintaining features during pre-training is the principle obstacle to the generalised pre-training necessary for foundation graph models. We have shown that pre-training on multiple domains of topologies offers significant performance improvements on downstream tasks (Hypothesis 1). In-fact we show entirely positive transfer across a wide range of domains and tasks

using adversarially pre-trained models with FoTOM.

Further, our results show that exposure to a larger variety of graph structures actually benefits performance. In Table 2, assuming that the Chem model has the least varied training data, then the Social model, then finally the All model, we can see that performance increases along the same order (Hypothesis 2). Performance between the Social and All models is highly comparable, despite the All model having double the training samples. We expect, though we leave this as an area for future research, that a yet greater breadth of domains in the pre-training data would bring greater performance benefits.

Hypothesis 2 in particular is significant, as the most intuitive assumption would be that exposing a molecular representation learner to non-molecular graphs would hinder its

performance. In other words we'd normally expect that this out-of-domain data would act as noise. Instead the Social and All models out-perform the Chem model on most molecular datasets under fine-tuning. Similarly one might expect that including node labels during fine-tuning (or supervised training of a non-pretrained model) would likely lead to these domain-specific models out-performing all-domain models. Our results instead show that performance is both superior and more consistent from our all-domain model on labelled molecular graphs, with performance increasing compared to the same model on non-labelled graphs. This in turn suggests that further features could be included in fine-tuning without performance loss.

5.2. Use-Cases

Given these findings the reasonable use-cases for this pre-trained model are broad. This potential benefit is two-fold. Firstly, pre-training and fine-tuning carries the normal decrease in expected training time. Secondly, as shown by our results in this work, our pre-trained models offer actual performance increase over simple supervised training. Our assumption is that the broad range of generic topological features learnt by the FoTOM model provide a more robust foundation for training than simple random initialisation, so pre-trained models avoid overfitting to non-useful features better than randomly initialised models. Guarantees on this point are left as an area for future research.

5.3. Assumptions, Risks, Future Directions

The most significant assumption we made - that a model can learn representations that are useful on multiple domains of downstream tasks - has been justified by our results above. However, in the full scope of downstream tasks for graph data, this first exploratory work is still fairly limited. Firstly we do not experiment with different graph augmentations (or "views"), instead employing only node and edge dropping. While we've shown that adversarial augmentations do improve pre-training, adversarial augmentations could be developed that include some of the greater complexities present in Hassani and Khasahmadi (2020), for example edge addition alongside edge dropping. We anticipate that a variety of augmentations, paired with a more detailed study of how different compositions of domain data influence representations, could bolster the expressivity of these topology-pre-trained models.

Secondly our experiments are limited to a few set compositions of domains. The non-task-specific evaluation of representation models is a challenging and open research problem. The same challenge is compounded on the large and high-dimensional graph space, which in comparison to other data structures both lacks intuitive human understanding and has a far smaller body of existing research.

The usual workaround for this issue is simply increasing the scale and breadth of the pre-training data (Russakovsky et al., 2015). Future work using FoTOM is highly likely to follow this same path. Additionally we restrict evaluation to graph-level tasks for simplicity. We anticipate that future work will evaluate FoTOM models on node and edge related tasks like classification and edge prediction. Lastly and most significantly the work here is limited to labelled and un-labelled graphs, whereas most domains carry far more detailed features on nodes and edges. We view this as the most critical area for future research.

A recent work has proposed definitions for, and expected properties of, graph foundation models (Liu et al., 2023) specifically. Their broad definition, '*...benefit from the pre-training of broad graph data, and can be adapted to a wide range of downstream graph tasks*', is satisfied by FoTOM. The two further properties proposed by this work, emergence and homogenization, are less easy to demonstrate. Indeed the authors themselves note that how these properties manifest is an open question, and therefore we similarly leave investigating whether FoTOM exhibits these properties as an area for future research.

6. Conclusion

We have presented FoTOM, a method for generalised multi-domain pre-training of graph models. FoTOM relies on excluding node and edge features during pre-training.

Findings Through contrastive learning we use FoTOM to present the first graph foundation models. On 76% of downstream tasks from multiple domains we show significant ($P \leq 0.01$) positive transfer compared to a non-pre-trained model with the same architecture. Compared to a supervised baseline, where results are not significantly better, they are never significantly worse. At 95% confidence we observe an 8 to 40% reduction in error over this supervised baseline.

Additionally we show that under the node and edge feature exclusion used in FoTOM pre-training on a single target domain leads to at-best on-par, and on most tasks significantly worse ($P \leq 0.01$), performance compared to pre-training on multiple non-target domains. This clearly demonstrates that the variety provided by out-of-domain pre-training can hold more value than the status-quo in-domain pre-training.

Directions We anticipate that future work will focus on several key areas: **1)** Improved or tailored graph augmentation strategies. **2)** Investigation of domain weighting in dataset compositions. **3)** A larger pre-training dataset spanning a wider range of domains. **4)** Application on node-level and edge-level tasks. **5)** The inclusion of arbitrary node and edge features.

References

- Rishi Bommasani, Drew A. Hudson, Ehsan Adeli, Russ Altman, Simran Arora, Sydney von Arx, Michael S. Bernstein, Jeannette Bohg, Antoine Bosselut, Emma Brunskill, Erik Brynjolfsson, Shyamal Buch, Dallas Card, Rodrigo Castellon, Niladri Chatterji, Annie Chen, Kathleen Creel, Jared Quincy Davis, Dora Demszky, Chris Donahue, Moussa Doumbouya, Esin Durmus, Stefano Ermon, John Etchemendy, Kawin Ethayarajh, Li Fei-Fei, Chelsea Finn, Trevor Gale, Lauren Gillespie, Karan Goel, Noah Goodman, Shelby Grossman, Neel Guha, Tatsunori Hashimoto, Peter Henderson, John Hewitt, Daniel E. Ho, Jenny Hong, Kyle Hsu, Jing Huang, Thomas Icard, Saahil Jain, Dan Jurafsky, Pratyusha Kalluri, Siddharth Karamcheti, Geoff Keeling, Fereshte Khani, Omar Khattab, Pang Wei Koh, Mark Krass, Ranjay Krishna, Rohith Kuditipudi, Ananya Kumar, Faisal Ladhak, Mina Lee, Tony Lee, Jure Leskovec, Isabelle Levent, Xiang Lisa Li, Xuechen Li, Tengyu Ma, Ali Malik, Christopher D. Manning, Suvir Mirchandani, Eric Mitchell, Zanele Munyikwa, Suraj Nair, Avani Narayan, Deepak Narayanan, Ben Newman, Allen Nie, Juan Carlos Niebles, Hamed Nilforoshan, Julian Nyarko, Giray Ogun, Laurel Orr, Isabel Papadimitriou, Joon Sung Park, Chris Piech, Eva Portelance, Christopher Potts, Aditi Raghunathan, Rob Reich, Hongyu Ren, Frieda Rong, Yusuf Roohani, Camilo Ruiz, Jack Ryan, Christopher Ré, Dorsa Sadigh, Shiori Sagawa, Keshav Santhanam, Andy Shih, Krishnan Srinivasan, Alex Tamkin, Rohan Taori, Armin W. Thomas, Florian Tramèr, Rose E. Wang, William Wang, Bohan Wu, Jiajun Wu, Yuhuai Wu, Sang Michael Xie, Michihiro Yasunaga, Jiaxuan You, Matei Zaharia, Michael Zhang, Tianyi Zhang, Xikun Zhang, Yuhui Zhang, Lucia Zheng, Kaitlyn Zhou, and Percy Liang. 2021. On the Opportunities and Risks of Foundation Models. *arXiv Preprint* 1, 1 (8 2021), 1–214. <https://arxiv.org/abs/2108.07258v3>
- Tom B Brown, Benjamin Mann, Nick Ryder, Melanie Subbiah, Jared Kaplan, Prafulla Dhariwal, Arvind Neelakantan, Pranav Shyam, Girish Sastry, Amanda Askell, Sandhini Agarwal, Ariel Herbert-Voss, Gretchen Krueger, Tom Henighan, Rewon Child, Aditya Ramesh, Daniel M Ziegler, Jeffrey Wu, Clemens Winter, Christopher Hesse, Mark Chen, Eric Sigler, Mateusz Litwin, Scott Gray, Benjamin Chess, Jack Clark, Christopher Berner, Sam McCandlish, Alec Radford, Ilya Sutskever, and Dario Amodei. 2020. Language Models are Few-Shot Learners. In *Advances in Neural Information Processing Systems*, H. Larochelle and M. Ranzato and R. Hadsell and M.F. Balcan and H. Lin (Ed.), Vol. 33. Curran Associates, Inc., 1877–1901. <https://commoncrawl.org/the-data/>
- Fenixiao Chen, Yun Cheng Wang, Bin Wang, and C. C. Jay Kuo. 2020. Graph representation learning: A survey. , e15 pages. <https://doi.org/10.1017/ATSIP.2020.13>
- Guanyi Chu, Xiao Wang, Chuan Shi, and Xunqiang Jiang. 2021. CuCo: Graph Representation with Curriculum Contrastive Learning.. In *IJCAI*, Zhi-Hua Zhou (Ed.). International Joint Conferences on Artificial Intelligence Organization, 2300–2306.
- Competition and Markets Authority. 2023. AI Foundation Models: Initial report - GOV.UK. <https://www.gov.uk/government/publications/ai-foundation-models-initial-report>
- Alex Davies and Nirav Ajmeri. 2022. Realistic Synthetic Social Networks with Graph Neural Networks. *arXiv Pre-Print* 1, 1 (12 2022), 1–12. <http://arxiv.org/abs/2212.07843>
- P. Erdos and A. Renyi. 1960. ON THE EVOLUTION OF RANDOM GRAPHS. (1960).
- Hakim Hafidi, Mounir Ghogho, Philippe Ciblat, and Ananthram Swami. 2022. Negative sampling strategies for contrastive self-supervised learning of graph representations. *Signal Processing* 190 (2022), 108310.
- William L Hamilton. 2020. Graph Representation Learning. *Synthesis Lectures on Artificial Intelligence and Machine Learning* 14, 3 (2020), 1–159.
- William L. Hamilton, Rex Ying, and Jure Leskovec. 2017. Representation Learning on Graphs: Methods and Applications. *arXiv* 1, 1 (9 2017), 1–24. <http://arxiv.org/abs/1709.05584>
- Kaveh Hassani and Amir Hosein Khasahmadi. 2020. Contrastive multi-view representation learning on graphs. *International conference on machine learning* 119, 1 (2020), 4116–4126.
- Weihua Hu, Bowen Liu, Joseph Gomes, Marinka Zitnik, Percy Liang, Vijay Pande, and Jure Leskovec. 2020. Strategies for Pre-training Graph Neural Networks. In *Proceedings of the 8th International Conference on Learning Representations (ICLR)*. International Conference on Learning Representations, ICLR.
- Shima Khoshraftar, Aijun An, Shima Khoshraftar, and Aijun An. 2022. A Survey on Graph Representation Learning Methods. *arXiv* 1, 1 (2022), arXiv:2204.01855. <https://doi.org/10.48550/ARXIV.2204.01855>
- Jure Leskovec, Kevin J. Lang, Anirban Dasgupta, and Michael W. Mahoney. 2009. Community structure in large networks: Natural cluster sizes and the absence of

- large well-defined clusters. *Internet Mathematics* 6, 1 (1 2009), 29–123. <https://doi.org/10.1080/15427951.2009.10129177>
- Haoyang Li, Xin Wang, Ziwei Zhang, Zehuan Yuan, Hang Li, and Wenwu Zhu. 2021. Disentangled contrastive learning on graphs. *Advances in Neural Information Processing Systems* 34 (2021), 21872–21884.
- Jiawei Liu, Cheng Yang, Zhiyuan Lu, Junze Chen, Yibo Li, Mengmei Zhang, Ting Bai, Yuan Fang, Lichao Sun, Philip S. Yu, and Chuan Shi. 2023. Towards Graph Foundation Models: A Survey and Beyond. *arXiv* 1, 1 (10 2023), 1–35. <http://arxiv.org/abs/2310.11829>
- Andrew Kachites McCallum, Kamal Nigam, Jason Rennie, and Kristie Seymore. 2000. Automating the construction of internet portals with machine learning. *Information Retrieval* 3, 2 (2000), 127–163. <https://doi.org/10.1023/A:1009953814988/METRICS>
- Robin Rombach, Andreas Blattmann, Dominik Lorenz, Patrick Esser, and Björn Ommer. 2022. High-Resolution Image Synthesis with Latent Diffusion Models. In *Proceedings of the IEEE/CVF Conference on Computer Vision and Pattern Recognition (CVPR)*. IEEE, New Orleans, 10684–10695. <https://github.com/CompVis/latent-diffusion>
- Benedek Rozemberczki, Carl Allen, and Rik Sarkar. 2021. Multi-Scale attributed node embedding. *Journal of Complex Networks* 9, 2 (5 2021), 1–22. <https://doi.org/10.1093/comnet/cnab014>
- Benedek Rozemberczki, Oliver Kiss, and Rik Sarkar. 2020. Karate Club: An API Oriented Open-source Python Framework for Unsupervised Learning on Graphs. In *CIKM '20: Proceedings of the 29th ACM International Conference on Information & Knowledge Management*. ACM, Online, Ireland, 3125–3132. <http://arxiv.org/abs/2003.04819>
- Olga Russakovsky, Jia Deng, Hao Su, Jonathan Krause, Sanjeev Satheesh, Sean Ma, Zhiheng Huang, Andrej Karpathy, Aditya Khosla, Michael Bernstein, Alexander C. Berg, and Li Fei-Fei. 2015. ImageNet Large Scale Visual Recognition Challenge. *International Journal of Computer Vision* 115, 3 (12 2015), 211–252. <https://doi.org/10.1007/S11263-015-0816-Y/FIGURES/16>
- Pascal Schweitzer PASCAL, Erik Jan van Leeuwen EJ-VANLEEUVEN, Nino Shervashidze, Pascal Schweitzer, Erik Jan van Leeuwen, Kurt Mehlhorn, Karsten M Borgwardt SHERVASHIDZE, and Van Leeuwen. 2011. Weisfeiler-Lehman Graph Kernels Nino Shervashidze Kurt Mehlhorn Karsten M. Borgwardt. *Journal of Machine Learning Research* 12, 1 (2011), 2539–2561.
- Hamed Shirzad, Kaveh Hassani, and Danica J. Sutherland. 2022. Evaluating Graph Generative Models with Contrastively Learned Features. In *Advances in Neural Information Processing Systems*, Vol. 35. New Orleans, 7783–7795. <https://github.com/hamedl375/>
- Susheel Suresh, Pan Li, Cong Hao, Georgia Tech, and Jennifer Neville. 2021. Adversarial Graph Augmentation to Improve Graph Contrastive Learning. In *Advances in Neural Information Processing Systems*, Vol. 34. 15920–15933. <https://github.com/susheels/adgcl>
- Naftali Tishby and Noga Zaslavsky. 2015. Deep Learning and the Information Bottleneck Principle. *2015 IEEE Information Theory Workshop, ITW 2015* (3 2015), 1–5. <https://doi.org/10.1109/ITW.2015.7133169>
- Michael Winding, Benjamin D. Pedigo, Christopher L. Barnes, Heather G. Patsolic, Youngser Park, Tom Kazimiers, Akira Fushiki, Ingrid V. Andrade, Avinash Khandelwal, Javier Valdes-Aleman, Feng Li, Nadine Randel, Elizabeth Barsotti, Ana Correia, Richard D. Fetter, Volker Hartenstein, Carey E. Priebe, Joshua T. Vogelstein, Albert Cardona, and Marta Zlatic. 2023. The connectome of an insect brain. *Science* 379, 6636 (3 2023). <https://doi.org/10.1126/science.add9330>
- Zhenqin Wu, Bharath Ramsundar, Evan N. Feinberg, Joseph Gomes, Caleb Geniesse, Aneesh S. Pappu, Karl Leswing, and Vijay Pande. 2017. MoleculeNet: A Benchmark for Molecular Machine Learning. *Chemical Science* 9, 2 (3 2017), 513–530. <https://doi.org/10.1039/c7sc02664a>
- Yuning You, Tianlong Chen, Yongduo Sui, Ting Chen, Zhangyang Wang, and Yang Shen. 2020. Graph contrastive learning with augmentations. *Advances in neural information processing systems* 33 (2020), 5812–5823.
- Ziwei Zhang, Haoyang Li, Zeyang Zhang, Yijian Qin, Xin Wang, and Wenwu Zhu. 2023. Graph Meets LLMs: Towards Large Graph Models. *arXiv Preprint* (8 2023). <https://arxiv.org/abs/2308.14522v2>
- Han Zhao, Xu Yang, Cheng Deng, and Dacheng Tao. 2023. Unsupervised Structure-Adaptive Graph Contrastive Learning. *IEEE Transactions on Neural Networks and Learning Systems* (2023). <https://doi.org/10.1109/TNNLS.2023.3271140>
- Jie Zhou, Ganqu Cui, Shengding Hu, Zhengyan Zhang, Cheng Yang, Zhiyuan Liu, Lifeng Wang, Changcheng

Li, and Maosong Sun. 2020. Graph neural networks: A review of methods and applications. *AI Open* 1 (1 2020), 57–81. <https://doi.org/10.1016/J.AIOPEN.2021.01.001>

Yanqiao Zhu, Yichen Xu, Qiang Liu, and Shu Wu. 2021. An empirical study of graph contrastive learning. *arXiv preprint arXiv:2109.01116* (2021).

A. Supplemental Material

On the combined encodings of the validation sets we compute R^2 correlation coefficients between the first five principal components (PCA) and common graph-level metrics. High correlations, or the lack thereof, should give some indication of how embedding components represent different graph characteristics.

The results are presented, along with each component's explained variance, in Table 3 and visualised in Figure 5.]

A Foundation Graph Model

Table 3: PCA components, fit on the embeddings of the test set, and their most correlated graph-level metric, for each of the trained models. **Underlined** text indicates a strong correlation $|R^2| \geq 0.66$, and **bold** text indicates moderate correlation $0.33 \leq |R^2| \leq 0.66$. We show up to the first five PCA components, but include only three where explained variance values are minimal.

	Variance Ratio	Metric Correlations					
		Most	R^2	Second	R^2	Third	R^2
Untrained							
PCA 0	9.96×10^{-01}	Number of Edges	0.219	Transitivity	0.072	Density	0.063
PCA 1	3.52×10^{-03}	Number of Edges	-0.555	Transitivity	-0.276	Density	-0.243
PCA 2	1.13×10^{-04}	Number of Edges	0.390	Transitivity	0.224	Density	0.210
Chem							
PCA 0	9.97×10^{-01}	Number of Edges	0.223	Transitivity	0.074	Density	0.065
PCA 1	2.60×10^{-03}	Number of Edges	-0.514	Transitivity	-0.253	Density	-0.225
PCA 2	1.14×10^{-05}	Number of Edges	0.132	Number of Nodes	0.051	Transitivity	0.047
Social							
PCA 0	9.99×10^{-01}	Number of Edges	0.127	Transitivity	0.032	Density	0.032
PCA 1	9.92×10^{-04}	Number of Nodes	1.00	Number of Edges	0.528	Density	-0.393
PCA 2	4.79×10^{-08}	Number of Edges	0.133	Density	0.070	Transitivity	0.054
All							
PCA 0	7.04×10^{-01}	Number of Nodes	0.999	Number of Edges	0.534	Density	-0.388
PCA 1	1.94×10^{-01}	Number of Edges	0.805	Density	0.737	Diameter	-0.554
PCA 2	4.23×10^{-02}	Average Clustering	0.309	Transitivity	0.248	Number of Edges	0.235
PCA 3	2.43×10^{-02}	Diameter	0.500	Average Clustering	-0.416	Transitivity	-0.243
PCA 4	1.82×10^{-02}	Density	-0.132	Transitivity	-0.108	Diameter	-0.088

Table 4: Scores for linear models applied to the encodings of each validation dataset, with and without node labels. For the classification datasets (ogbg-molclintox and Twitch Egos) we report AUROC, other datasets report RMSE. Some datasets, where results are very similar for each model, are excluded. **Bold** text indicates a superior result. For clarity the results for a given dataset are scaled by a constant factor.

	Untrained	Chem	Social	All	Magnitude
molreesolv	4.21 ± 4.13	3130 ± 5990	2.00 ± 0.869	1.01 ± 1.02	10^3
molesol	48.3 ± 90.2	817 ± 1150	48.1 ± 62.9	28.1 ± 38.1	10^0
mollipo	29.4 ± 17.9	14.9 ± 2.0	4.45 ± 0.62	5.33 ± 0.56	10^0
molclintox	0.487 ± 0.005	0.440 ± 0.007	0.500 ± 0.000	0.500 ± 0.000	10^0
Facebook	10.6 ± 1.7	10.7 ± 20	7.73 ± 1.87	4.44 ± 5	10^{-3}
Twitch Egos	0.638 ± 0.012	0.610 ± 0.072	0.679 ± 0.002	0.694 ± 0.002	10^0
Roads	263 ± 0.5	256 ± 0.0	298 ± 0.3	2.85 ± 5	10^{-5}
Trees	7.66 ± 0.16	2.85 ± 0.0	2.98 ± 0.03	2.56 ± 0.05	10^{-3}
Community	4.36 ± 0.05	4.25 ± 0.00	12.0 ± 2	4.46 ± 0.07	10^{-5}
Random	6.46 ± 0.7	3.27 ± 0.0	1.20 ± 0.2	3.38 ± 0.0	10^{-4}
	Untrained-Labels	Chem-Labels	Social-Labels	All-Labels	
molreesolv	480 ± 172	$(1.13 \pm 0.64) \times 10^6$	90900 ± 83300	11000 ± 5600	10^0
molesol	29.4 ± 7.8	18.5 ± 7.3	531 ± 292	34.1 ± 33.0	10^0
mollipo	7.33 ± 1.37	7.25 ± 1.01	4.02 ± 0.92	5.01 ± 0.53	10^0
molclintox	0.511 ± 0.022	0.497 ± 0.001	0.428 ± 0.001	0.526 ± 0.060	10^0
Facebook	14.6 ± 11.1	10.8 ± 1.1	7.82 ± 1.9	4.43 ± 6	10^{-3}

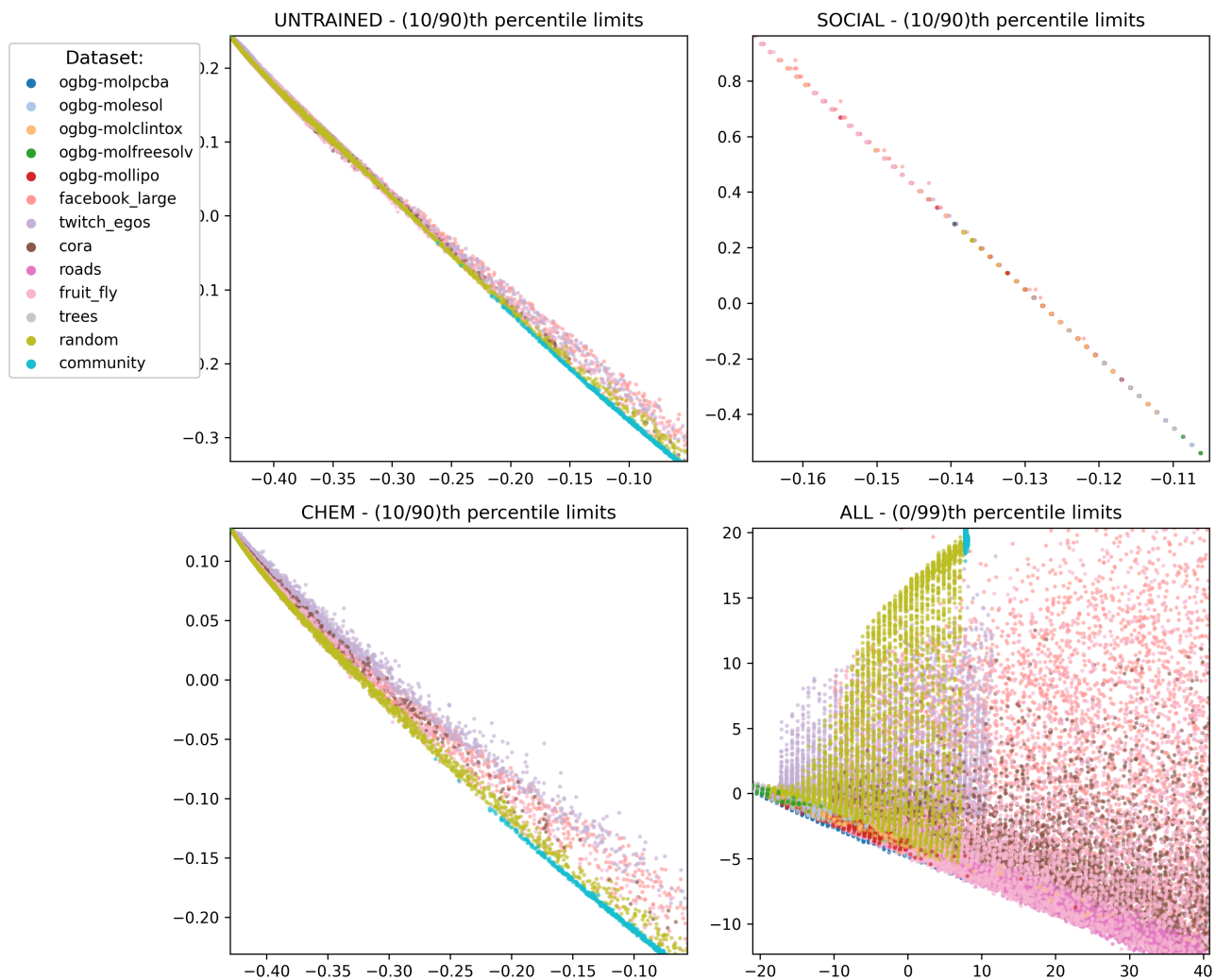


Figure 4: PCA projections of encodings from each model, as well as an untrained model. We scale axes by percentiles - of - data - included as for all except the All model the projections have outliers in the region 10^7 .

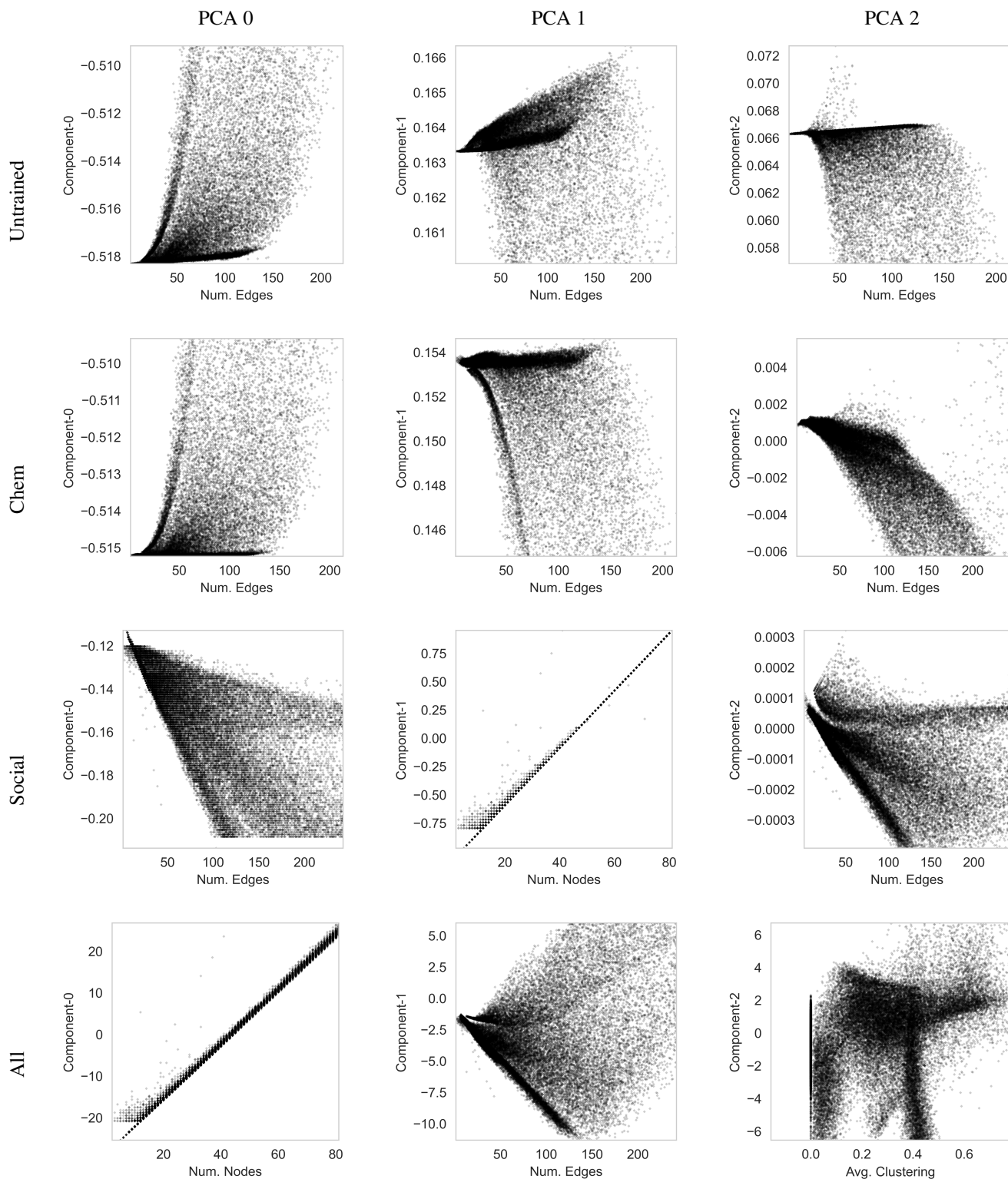


Figure 5: PCA components of the encodings of each model across the whole validation dataset, scattered against the most correlated metrics, as in Table 3.

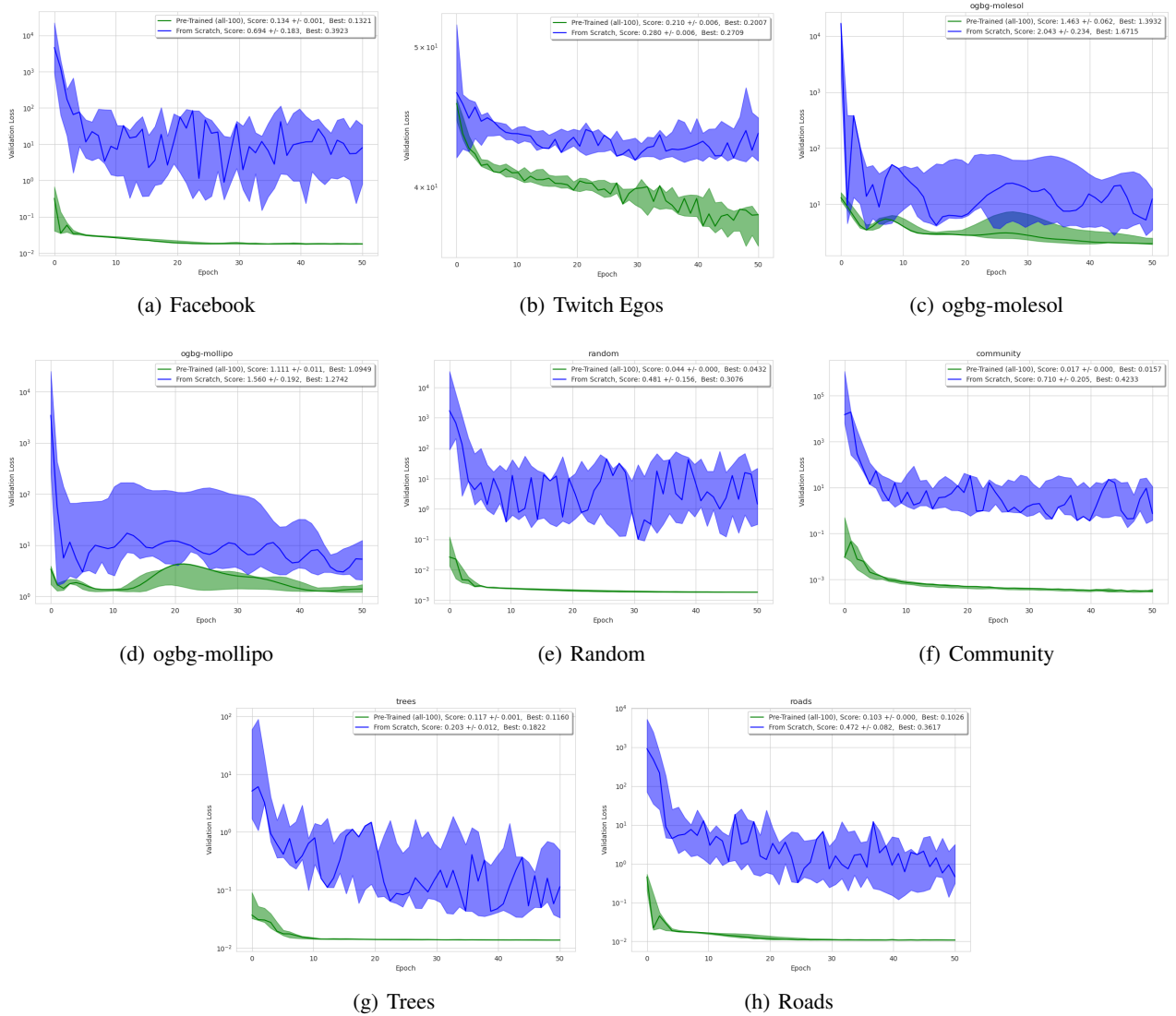


Figure 6: Validation scores for fine-tuning on a subset of our training datasets. The Twitch dataset carries its binary classification task and so we report 1 - AUROC. On other datasets tasks are regression, and we report MSE.

Table 5: Scores for fine-tuning models trained with **random node dropping** on each validation dataset, with (**Model**-labels) and without (**Model**) node labels. For the classification datasets (ogbg-molclintox and Twitch Egos) we report AUROC, other datasets report RMSE. Some datasets, where results are very similar for each model, are excluded. **Bold** text indicates a result beats the unsupervised (GIN) baseline. **Underlined** text indicates a superior result, down to three significant figures. GIN results are duplicated from Table 2.

	GIN	Chem	Social	All
molreesolv	4.978 ± 0.479	<u>3.838 ± 0.120</u>	4.041 ± 0.116	4.157 ± 0.138
molesol	1.784 ± 0.094	1.897 ± 0.075	1.520 ± 0.066	<u>1.357 ± 0.037</u>
mollipo	1.143 ± 0.031	1.123 ± 0.105	1.015 ± 0.013	<u>0.983 ± 0.015</u>
molclintox	<u>0.530 ± 0.042</u>	0.469 ± 0.030	0.431 ± 0.002	0.530 ± 0.086
molbbbp	<u>0.565 ± 0.043</u>	0.497 ± 0.027	0.548 ± 0.037	0.567 ± 0.032
molbase	0.677 ± 0.053	0.740 ± 0.026	0.686 ± 0.055	0.679 ± 0.067
molhiv	0.355 ± 0.059	0.283 ± 0.001	0.635 ± 0.046	0.644 ± 0.039
Facebook	0.311 ± 0.065	0.261 ± 0.101	0.159 ± 0.015	0.145 ± 0.012
Twitch Egos	0.72 ± 0.006	0.460 ± 0.041	0.744 ± 0.006	0.743 ± 0.003
Roads	0.46 ± 0.073	0.228 ± 0.118	0.150 ± 0.015	0.132 ± 0.018
Trees	0.203 ± 0.012	0.415 ± 0.250	0.135 ± 0.015	0.125 ± 0.009
Community	0.743 ± 0.106	0.084 ± 0.083	0.080 ± 0.018	0.074 ± 0.021
Random	0.529 ± 0.228	0.123 ± 0.075	0.076 ± 0.010	0.058 ± 0.005
	GIN-Labels	Chem-Labels	Social-Labels	All-Labels
molreesolv	4.854 ± 0.513	<u>3.819 ± 0.136</u>	4.113 ± 0.070	3.984 ± 0.162
molesol	1.707 ± 0.073	1.809 ± 0.139	1.480 ± 0.067	<u>1.378 ± 0.031</u>
mollipo	1.143 ± 0.031	1.182 ± 0.128	<u>0.986 ± 0.017</u>	0.997 ± 0.011
molclintox	<u>0.497 ± 0.038</u>	0.474 ± 0.036	0.430 ± 0.002	0.474 ± 0.056
molbbbp	<u>0.561 ± 0.034</u>	0.491 ± 0.032	0.543 ± 0.016	0.565 ± 0.036
molbase	0.698 ± 0.050	0.751 ± 0.024	0.677 ± 0.030	0.675 ± 0.088
molhiv	0.374 ± 0.052	0.286 ± 0.008	0.615 ± 0.047	0.628 ± 0.044
Facebook	0.749 ± 0.250	0.354 ± 0.166	0.151 ± 0.016	0.156 ± 0.022
Superior Result	19.0%	19.0%	19.0%	61.9%
Beats Baseline	-	47.6%	76.2%	90.5%

Table 6: Scores for fine-tuning models trained with **random edge dropping** on each validation dataset, with (**Model**-labels) and without (**Model**) node labels. For the classification datasets (ogbg-molclintox and Twitch Egos) we report AUROC, other datasets report RMSE. Some datasets, where results are very similar for each model, are excluded. **Bold** text indicates a result beats the unsupervised (GIN) baseline. **Underlined** text indicates a superior result, down to three significant figures. GIN results are duplicated from Table 2.

	GIN	Chem	Social	All
molfreeolv	4.978 ± 0.479	134.800 ± 225.200	<u>4.102 ± 0.049</u>	4.197 ± 0.095
molesol	1.784 ± 0.094	14.050 ± 23.760	<u>1.312 ± 0.094</u>	1.571 ± 0.059
mollipo	1.129 ± 0.040	1.034 ± 0.029	<u>0.989 ± 0.011</u>	1.068 ± 0.026
molclintox	0.530 ± 0.042	0.449 ± 0.013	0.426 ± 0.006	0.461 ± 0.029
molbbbp	0.565 ± 0.043	0.570 ± 0.040	<u>0.602 ± 0.025</u>	0.603 ± 0.029
molbace	0.677 ± 0.053	0.768 ± 0.006	<u>0.783 ± 0.045</u>	0.756 ± 0.030
molhiv	0.355 ± 0.059	0.576 ± 0.152	<u>0.647 ± 0.066</u>	0.501 ± 0.135
Facebook	0.311 ± 0.065	3.70 ± 6.95	<u>0.180 ± 0.019</u>	0.237 ± 0.063
Twitch Egos	0.72 ± 0.006	0.717 ± 0.005	<u>0.753 ± 0.006</u>	0.739 ± 0.007
Roads	0.46 ± 0.073	<u>0.156 ± 0.007</u>	<u>0.167 ± 0.039</u>	0.252 ± 0.029
Trees	0.203 ± 0.012	<u>0.143 ± 0.009</u>	0.161 ± 0.019	0.187 ± 0.020
Community	0.743 ± 0.106	<u>0.014 ± 0.000</u>	0.146 ± 0.024	0.314 ± 0.069
Random	0.529 ± 0.228	<u>0.055 ± 0.012</u>	0.107 ± 0.019	0.289 ± 0.098
	GIN-Labels	Chem-Labels	Social-Labels	All-Labels
molfreeolv	4.854 ± 0.513	103.400 ± 232.200	<u>4.106 ± 0.021</u>	4.163 ± 0.069
molesol	1.707 ± 0.073	8.006 ± 7.850	<u>1.358 ± 0.028</u>	1.597 ± 0.069
mollipo	1.143 ± 0.031	1.043 ± 0.026	<u>0.995 ± 0.014</u>	1.063 ± 0.038
molclintox	0.497 ± 0.038	0.446 ± 0.020	0.422 ± 0.009	0.475 ± 0.031
molbbbp	0.561 ± 0.034	0.535 ± 0.079	<u>0.612 ± 0.015</u>	0.589 ± 0.031
molbace	0.698 ± 0.050	0.763 ± 0.018	<u>0.776 ± 0.032</u>	0.744 ± 0.034
molhiv	0.374 ± 0.052	0.632 ± 0.087	<u>0.652 ± 0.100</u>	0.479 ± 0.102
Facebook	0.749 ± 0.250	2.80 ± 4.14	<u>0.179 ± 0.020</u>	0.263 ± 0.067
Superior Result	9.5%	19.0%	71.4%	4.8%
Beats Baseline	-	52.4%	90.5%	90.5%

Table 7: Results for fine-tuning from each pre-training regime, data subset and model on the OGB (Open Graph Benchmark) single-target molecular datasets. Unlike other tables the classification datasets are reported 1-AUROC for improved clarity. **Underlined** results are superior. **Bold** results out-perform the supervised (GIN) baseline.

Pre-Training	Data	Labels	molbac	molbbp	molcintox	molhiv	molresolv	molipo	moldep						
			± dev												
None	None	✓	0.323	0.053	0.435	0.043	0.47	0.645	0.059	1.784	0.094	4.978	0.479	1.129	0.04
None	None		0.302	0.05	0.439	0.034	0.503	0.626	0.052	1.707	0.073	4.854	0.513	1.143	0.031
Rand. Edge	CHEM	None	0.237	0.018	0.465	0.079	0.554	0.368	0.087	8.006	7.85	103.4	232.2	1.043	0.026
Rand. Edge	CHEM	✓	0.232	0.006	0.43	0.04	0.551	0.424	0.152	14.05	23.76	134.8	225.2	1.034	0.029
Rand. Edge	SOC.	None	0.217	0.045	0.398	0.025	0.574	0.353	0.066	1.312	0.094	4.102	0.049	0.989	0.011
Rand. Edge	SOC.	✓	0.224	0.032	0.388	0.015	0.578	0.348	0.1	1.358	0.028	4.106	0.021	0.995	0.014
Rand. Edge	ALL	None	0.244	0.03	0.397	0.029	0.539	0.499	0.135	1.571	0.059	4.197	0.095	1.068	0.026
Rand. Edge	ALL	✓	0.256	0.034	0.411	0.031	0.525	0.521	0.102	1.597	0.059	4.163	0.069	1.063	0.038
Rand. Node	CHEM	None	0.26	0.026	0.503	0.027	0.531	0.717	0.001	1.897	0.075	3.838	0.12	1.123	0.105
Rand. Node	CHEM	✓	0.249	0.024	0.509	0.032	0.526	0.714	0.008	1.809	0.139	3.819	0.136	1.182	0.128
Rand. Node	SOC.	None	0.314	0.055	0.452	0.037	0.569	0.365	0.046	1.52	0.066	4.041	0.116	1.015	0.013
Rand. Node	SOC.	✓	0.323	0.03	0.457	0.046	0.57	0.385	0.047	1.48	0.067	4.113	0.07	0.986	0.017
Rand. Node	ALL	None	0.321	0.067	0.423	0.032	0.470	0.356	0.039	1.357	0.037	4.157	0.138	0.983	0.015
Rand. Node	ALL	✓	0.325	0.088	0.435	0.036	0.536	0.372	0.044	1.378	0.031	3.984	0.162	0.997	0.011
AD-GCL	SOC.	None	0.255	0.025	0.4	0.026	0.499	0.36	0.047	1.472	0.042	3.829	0.114	0.989	0.01
AD-GCL	SOC.	✓	0.278	0.045	0.405	0.029	0.442	0.347	0.047	1.494	0.065	3.817	0.07	0.992	0.009
AD-GCL	CHEM	None	0.369	0.128	0.456	0.043	0.486	0.46	0.133	1.439	0.089	3.888	0.207	1.041	0.019
AD-GCL	CHEM	✓	0.406	0.11	0.449	0.042	0.483	0.531	0.098	1.46	0.079	3.825	0.123	1.074	0.033
AD-GCL	ALL	None	0.293	0.017	0.411	0.022	0.452	0.343	0.044	1.308	0.034	4.255	0.029	0.967	0.014
AD-GCL	ALL	✓	0.274	0.023	0.374	0.019	0.425	0.358	0.04	1.302	0.03	4.25	0.047	0.974	0.012

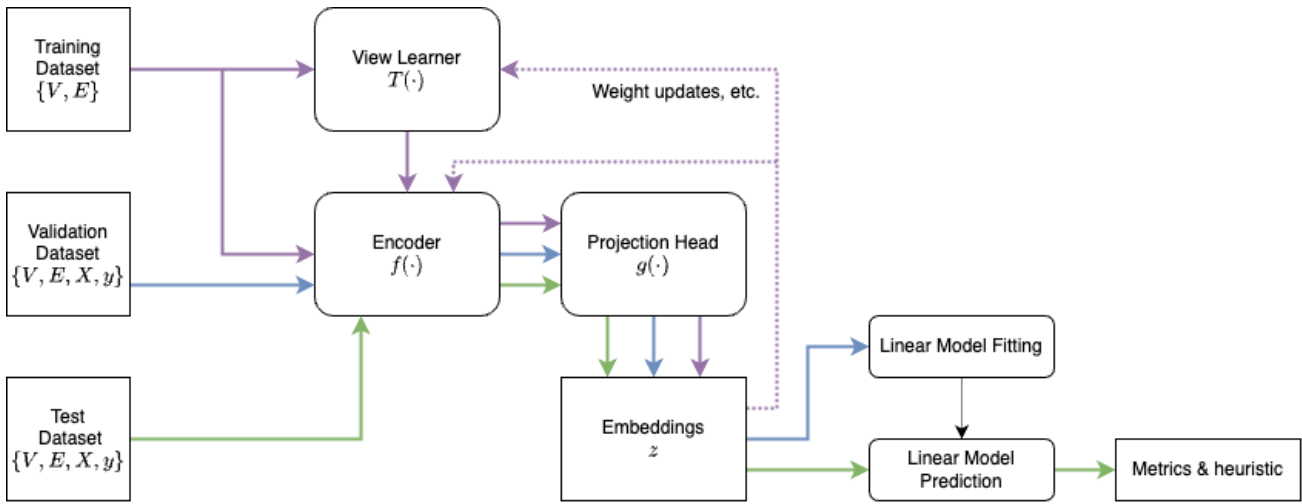


Figure 7: Our evaluation process. V represents nodes, E edges, X node labels (where available and if included) and y graph target values. Purple lines indicate processes involve testing data, blue involve validation data, and green involve test set data.

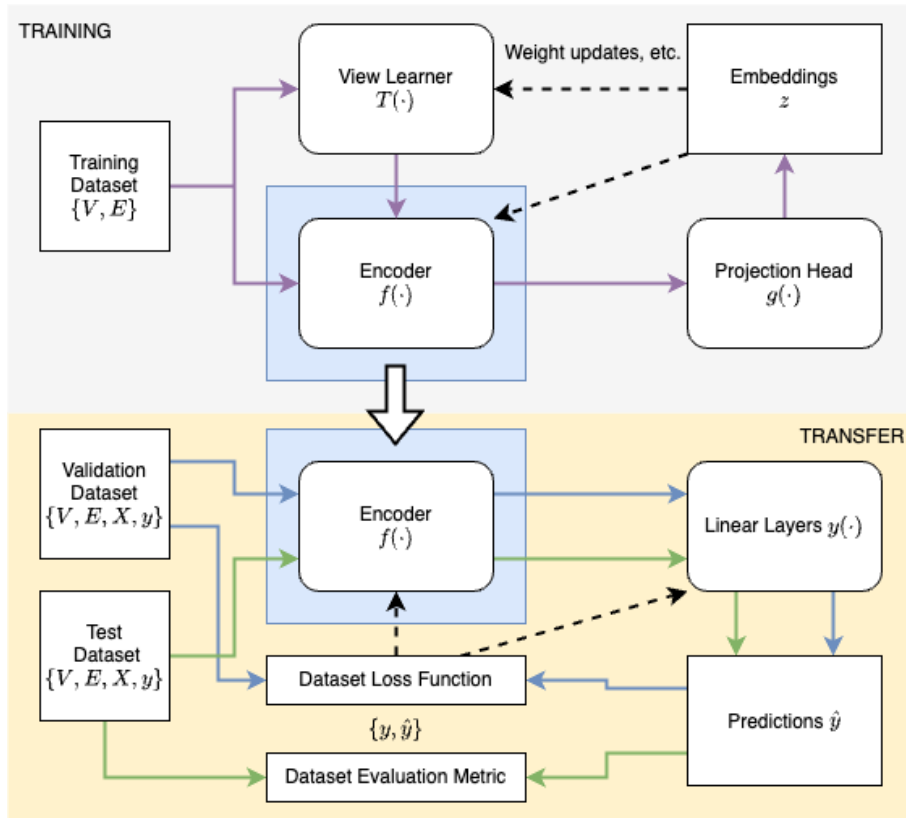


Figure 8: Our evaluation process for transfer learning. V represents nodes, E edges, X node labels (where available and if included) and y graph target values.

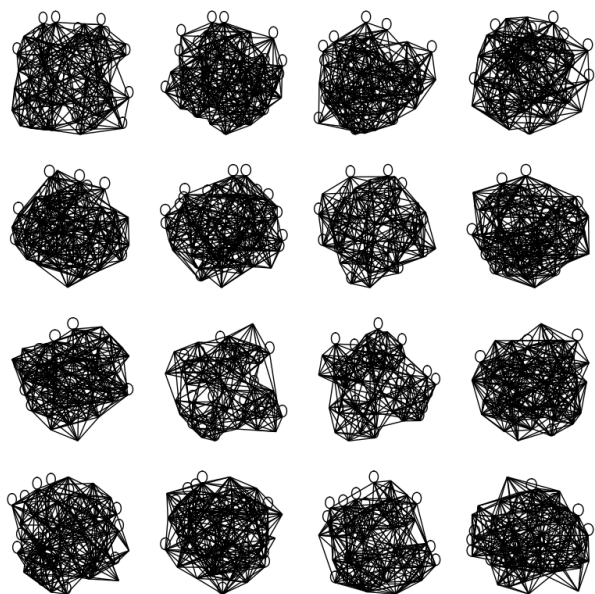


Figure 9: Graphs from the community dataset

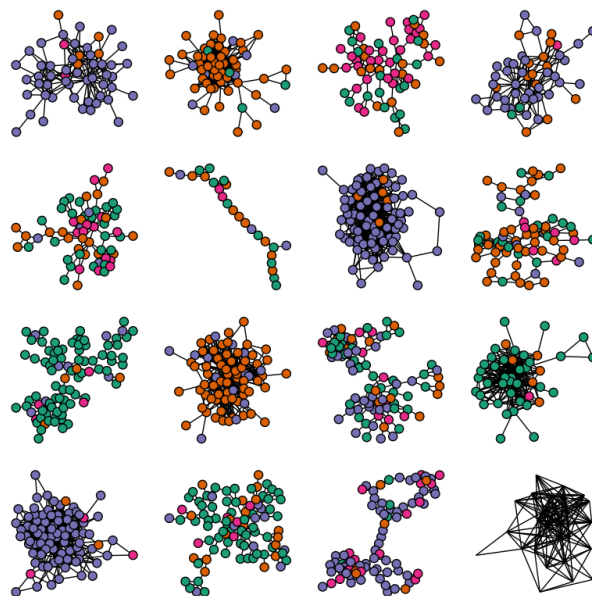


Figure 11: Graphs from the Facebook dataset (Rozemberczki et al., 2021)

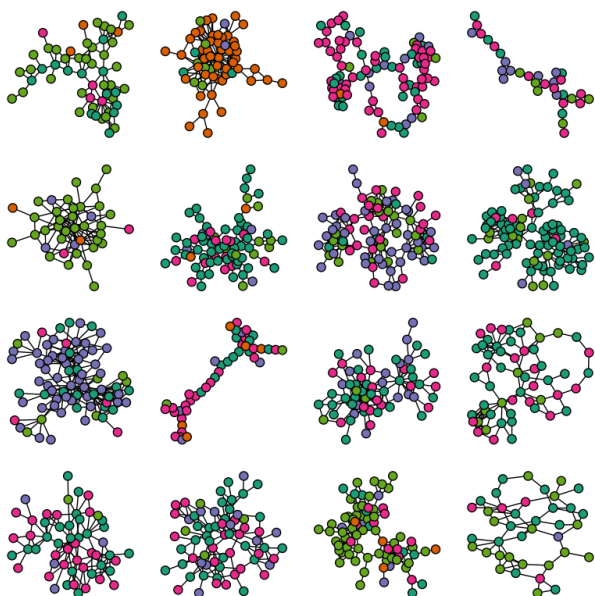


Figure 10: Graphs from the CORA dataset (McCallum et al., 2000)

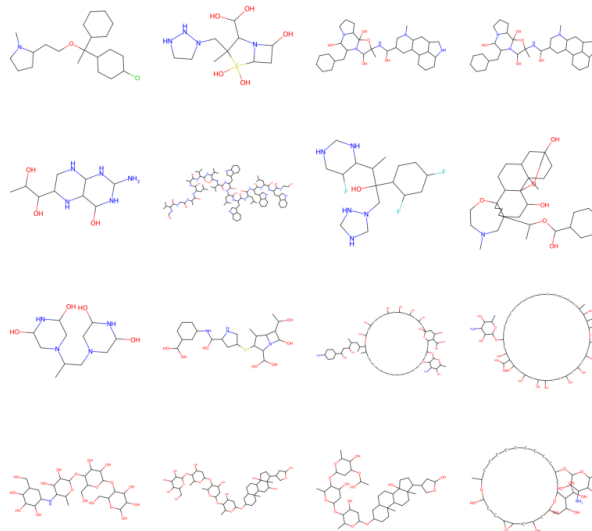


Figure 12: Graphs from the ogbg-molclintox dataset (Hu et al., 2020)

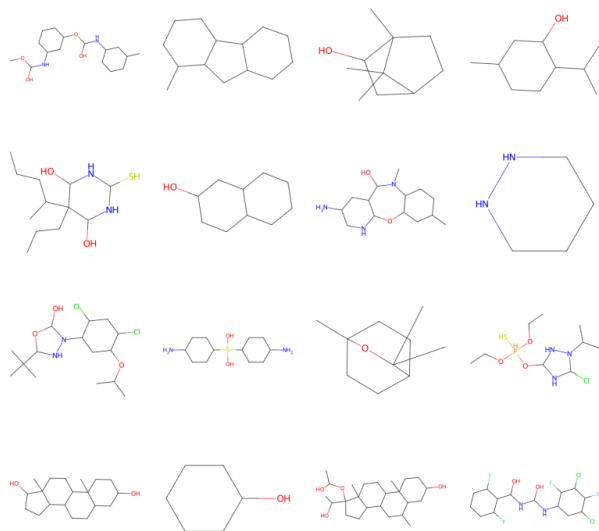


Figure 13: Graphs from the ogbg-molesol dataset (Hu et al., 2020)

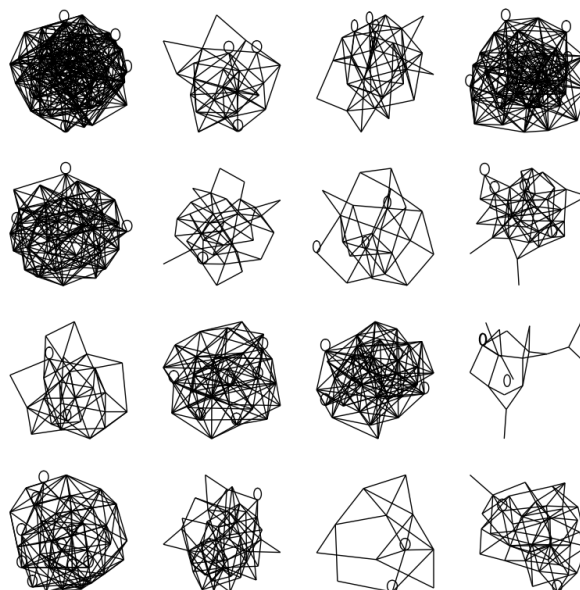


Figure 15: Graphs from the random dataset

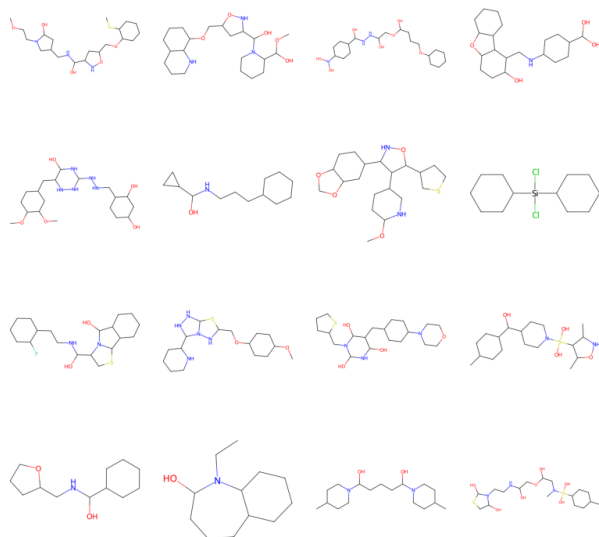


Figure 14: Graphs from the ogbg-molpcba dataset (Hu et al., 2020)

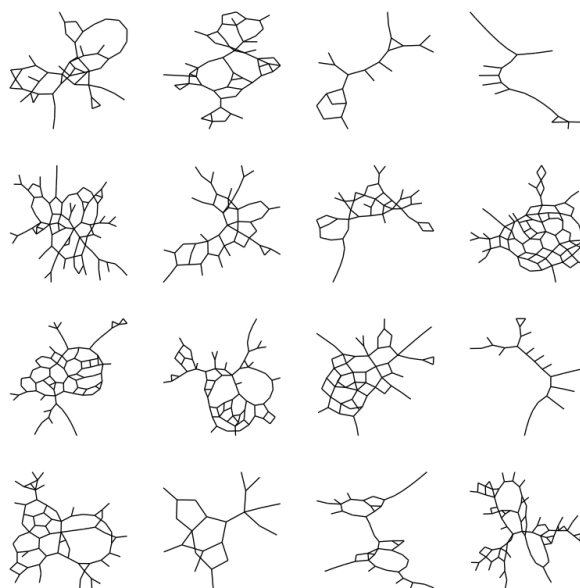


Figure 16: Graphs from the roads dataset (Leskovec et al., 2009)

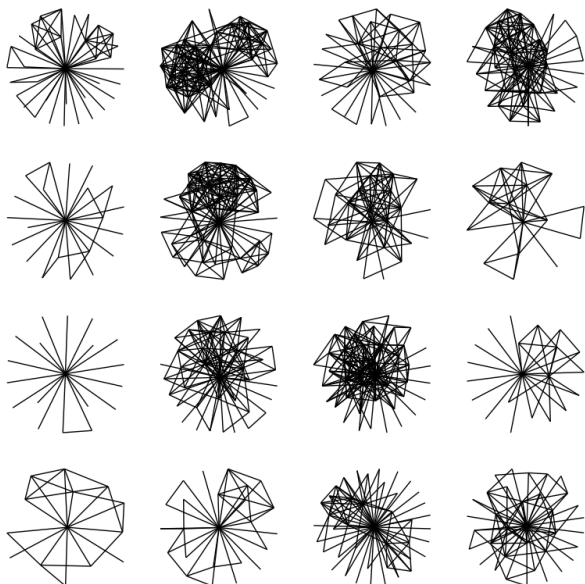


Figure 17: Graphs from the twitch egos dataset (Rozemberczki et al., 2020)

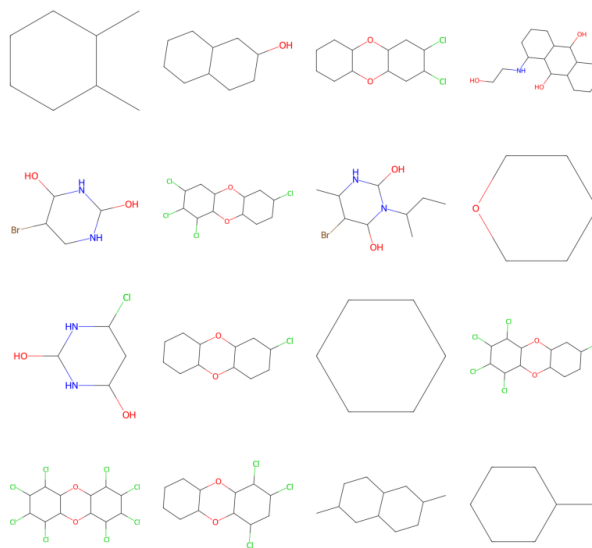


Figure 19: Graphs from the molfreeolv dataset (Hu et al., 2020)

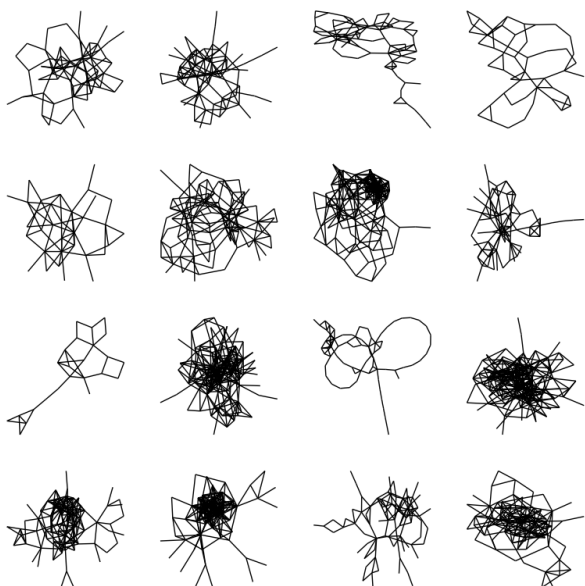


Figure 18: Graphs from the fruit fly brain dataset (Winding et al., 2023)

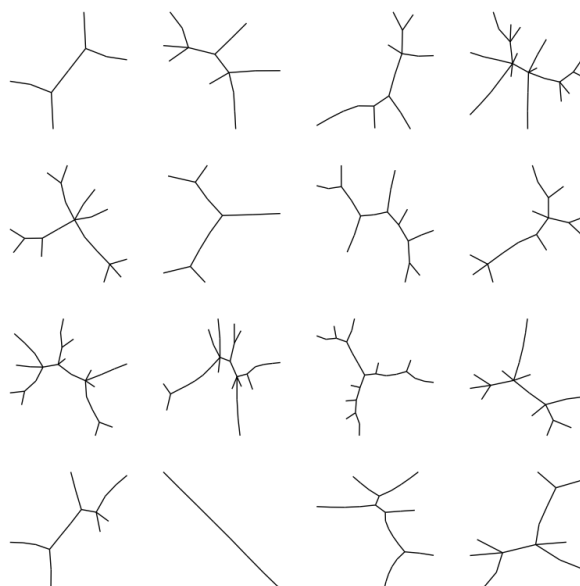


Figure 20: Graphs from the trees dataset

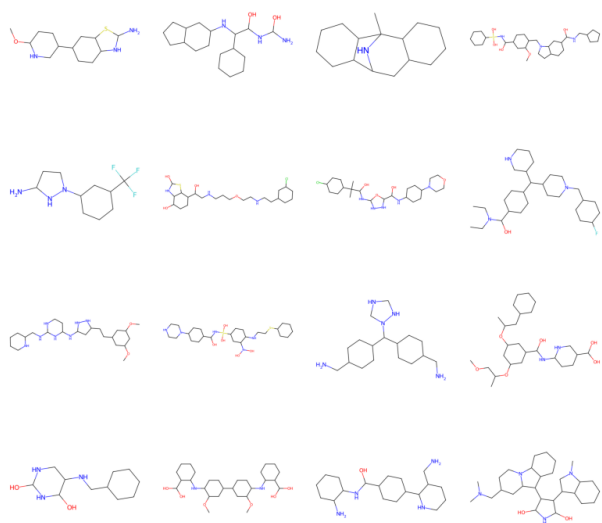


Figure 21: Graphs from the mollipo dataset (Hu et al., 2020)